Polarization density profiles for dipoles against an electrified wall in the MS and RLHNC approximations

Jayendran C. Rasaiah

Department of Chemistry and Laboratory for Surface Science and Technology, University of Maine, Orono, Maine 04469

Dennis J. Isbister

Department of Chemistry, University of New South Wales, RMC, Duntroon, ACT 2600, Australia

John Eggebrecht[a)]

Department of Chemistry, University of Maine, Orono, Maine 04469
(Received 1 June 1981; accepted 20 August 1981)

The polarization density profiles $\mathbf{P}(z, \mathbf{E})$ for dipoles in the vicinity of a wall, from which an electric field emerges, have been calculated using the mean spherical (MS) and renormalized linearized hypernetted chain (RLHNC) approximations. The profiles for the two approximations are significantly different. The presence of a component of the polarization density that is perpendicular to the field $\mathbf{E}$, when the field is neither perpendicular nor parallel to the wall, is noted. The anisotropic response of the fluid to the electric field in the vicinity of the wall is discussed in terms of a local dielectric tensor when the relationship between the polarization density and the electric field is linear.

I. INTRODUCTION

The polarization density $\mathbf{P}$ or dipole moment per unit volume is a fundamental property which enters into nearly every discussion of the dielectric properties of a fluid.[1] The well-known linear constitutive relation

$$\mathbf{P} = [(\epsilon - 1)/4\pi]\,\mathbf{E}\,, \tag{1.1}$$

which links $\mathbf{P}$ with the Maxwell field $\mathbf{E}$, defines a field independent dielectric constant ϵ in the limit of zero field. Recent studies of the density profiles of dipoles adsorbed at a wall[2,3] enable Eq. (1.1) to be extended in two ways. Firstly, it has been possible to discuss nonlinear contributions of $0(E^3)$ to $\mathbf{P}$ by employing the quadratic hypernetted chain (QHNC) approximation[4] for the wall particle correlation function, and secondly, we can, as we are about to show, obtain the polarization density profiles in much the same way that the density profiles for dipoles have already been determined in the mean spherical (MS) and renormalized linearized hypernetted chain (RLHNC) approximations.

In what follows we consider the polarization density of an open system bounded on one side by a flat wall from which an electric field emerges at an inclination α to the unit normal $\hat{n}$. The local polarization density is $\mathbf{P}(z, \mathbf{E}_2)$, where z is the distance from the wall and $\mathbf{E}_2$ is the external electric field. In our study, this field is created by a dipole embedded in a nonconducting hard sphere of infinite size thereby mimicking a flat hard wall from which an electric field emanates (see Fig. 1). The external field $\mathbf{E}_2$ is related to the inclination of the wall dipole by

$$\mathbf{E}_2 = E_0(3\cos^2\Theta_2 + 1)^{1/2}\,\hat{e}_2\,, \tag{1.2}$$

where E_0 is a constant, Θ_2 is the angle between a unit vector $\hat{s}_2$ in the direction of the wall dipole and the unit normal $\hat{n}$, and

$$\hat{e}_2 = \frac{3\cos\Theta_2\hat{n} - \hat{s}_2}{(3\cos^2\Theta_2 + 1)^{1/2}}\,, \tag{1.3}$$

where $\hat{e}_2$ is a unit normal in the direction of $\mathbf{E}_2$. The field $\mathbf{E}_2$ is independent of z and the relationship between α and Θ_2 is given by

$$\cos\alpha = \frac{2\cos\Theta_2}{(3\cos^2\Theta_2 + 1)^{1/2}}\,. \tag{1.4}$$

As discussed elsewhere,[4] the Maxwell field $\mathbf{E}$ and the external field $\mathbf{E}_2$ are related by

$$\mathbf{E} = \frac{3}{(2\epsilon + 1)}\,\mathbf{E}_2 + \text{nonlinear terms}\,, \tag{1.5}$$

where the coefficients beyond the linear term in Eq. (1.5) are one source of nonlinear effects in the polarization density $\mathbf{P}(\infty, \mathbf{E}_2)$ in an open system; the other is electrostriction.

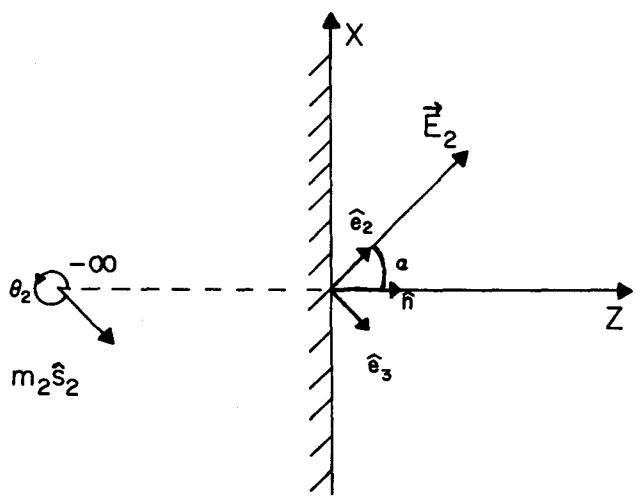

FIG. 1. The coordinate system used to describe the wall-dipole interactions, the electric field vector $\mathbf{E}_2$, and the wall dipole $m_2\,\hat{s}_2$.

[a)] Present address: School of Chemical Engineering, Olin Hall, Cornell University, Ithaca, N.Y. 14853.

 0021-9606/81/235497-06$01.00

The symmetry of the system allows $\mathbf{P}(z,\ \mathbf{E}_2)$ to be decomposed into two components, which we take to be parallel and perpendicular to the electric field $\mathbf{E}_2$ with unit vectors $\hat{e}_2$ and $\hat{e}_3$ along these directions so that $\hat{e}_3$ and $\hat{e}_2$ are a right-handed pair of coordinate axes in the plane defined by $\mathbf{E}_2$ and $\hat{n}$. We can, therefore, write

$$\mathbf{P}(z,\ \mathbf{E}_2) = \left|\mathbf{P}(\infty,\ \mathbf{E}_2)\right| \left[P_2(z,\ \alpha)\,\hat{e}_2 + P_3(z,\ \alpha)\hat{e}_3\right] , \tag{1.6}$$

with

$$\lim P_2(z,\ \alpha) = 1 , \quad z \to \infty , \tag{1.7}$$

$$\lim P_3(z,\ \alpha) = 0 , \quad z \to \infty , \tag{1.8}$$

which follows from the fact that $\mathbf{P}(\infty,\ \mathbf{E}_2)$, the polarization density infinitely far from the wall, is parallel to the electric field, when they are linearly related to each other. It has been shown elsewhere that $\mathbf{P}(\infty,\ \mathbf{E}_2)$ obeys the linear constitutive relation when the MS and LHNC approximation are used for the wall–particle correlation functions and when the nonlinear terms in Eq. (1.5) are neglected.[4]

This paper deals with the determination of the polarization density profiles $\mathbf{P}(z,\ \mathbf{E}_2)$ for the MS and RLHNC approximations through the calculation of $P_2(z,\ \alpha)$ and $P_3(z,\ \alpha)$ for $0 \leq \alpha \leq \pi/2$. For these approximations $P_2(z,\ \alpha)$ and $P_3(z,\ \alpha)$ are independent of the electric field, and merely serve to scale the field dependent $\mathbf{P}(\infty,\ \mathbf{E}_2)$ of Eq. (1.6) in determining the polarization density profiles. This is not the case with the QHNC approximation. Carnie and Chan[5] have also discussed polarization density profiles away from a flat charged wall but for ion–dipole mixtures (of low electrolyte concentration) using the MS approximation. The electric field that is employed is always perpendicular to the surface and is a function of the electrolyte concentration and the distance from the wall. The same system has also been studied by Blum and Henderson.[6] Our discussion, although limited to dipoles, includes a comparative study of the RLHNC and MS approximations. Although both these are linear approximations, the density and polarization density profiles that they predict are significantly different. We have also studied changes in these profiles brought about by altering the electric field angle, and find effects which have not to our knowledge, been explicitly calculated before. These special effects arise from the presence of a component of the polarization density that is perpendicular to the electric field and is related to $P_3(z,\ \alpha)$ in Eq. (1.6). This component vanishes at an infinite distance from the flat surface where the component in the direction of the field assumes the bulk value. When the field is parallel or perpendicular to the wall however, $P_3(z,\ \alpha)$ vanishes, and there is only a single component to the polarization density which is always parallel to the field. In the MS and LHNC (or RLHNC) approximations, the two profiles for fields parallel and perpendicular to the interface completely determine the components of the polarization density at any other field angle. The wall therefore introduces an anisotropic response to an external electric field, which may be discussed in terms of a local dielectric tensor when this response is linear. We conclude this section by recalling a few formulas, in the notation of Ref. 3, that are essential to our discussion.

The wall–particle correlation function $h_{21}(z,\ \mathbf{E}_2,\ \boldsymbol{\Omega}_1)$ has the invariant expansion

$$h_{21}(z,\ \mathbf{E}_2,\ \boldsymbol{\Omega}_1) = h_{21}^s(z) + h_{21}^D(z) D(2,\ 1) + h_{21}^{\Delta}(z)\,\Delta(2,\ 1) + \cdots , \tag{1.9}$$

with an analogous expansion for the direct correlation function $c_{21}(z,\ \mathbf{E}_2,\ \boldsymbol{\Omega}_1)$. In Eq. (1.9), the basis functions $D(2,\ 1)$ and $\Delta(2,\ 1)$ have the usual definitions:

$$D(2,\ 1) = \hat{s}_2 \cdot (3\hat{n}\hat{n} - \mathbf{U}) \cdot \hat{s}_1 , \tag{1.10}$$

$$\Delta(2,\ 1) = \hat{s}_2 \cdot \hat{s}_1 , \tag{1.11}$$

where $\hat{s}_2$ and $\hat{s}_1$ are unit vectors in the direction of the wall–dipole and fluid–dipole, respectively, and $\mathbf{U}$ is the unit tensor. The coefficient $h_{21}^{\Delta}(z)$ in Eq. (1.9) is short-ranged, while $h_{21}^D(z)$ is long-ranged and can be written as the sum of two terms

$$h_{21}^D(z) = \hat{h}_{21}^D(z) + 3K_{21} , \tag{1.12}$$

in which $\hat{h}_{21}^D(z)$ is a short-ranged function and K_{21} is a constant related to the electric field. The density profile $\rho_1(z,\ \mathbf{E}_2,\ \boldsymbol{\Omega}_1)$ of fluid dipoles against the wall is obtained from

$$\rho_1(z,\ \mathbf{E}_2,\ \boldsymbol{\Omega}_1) = \rho_1^0\left[1 + h_{21}(z,\ \mathbf{E}_2,\ \boldsymbol{\Omega}_1)\right] , \tag{1.13}$$

where ρ_1^0 is the density of the bulk fluid in the absence of the electric field.[4]

II. THE POLARIZATION DENSITY PROFILE

From the definition of the polarization density in the grand canonical ensemble we have[1]

$$\mathbf{P}(z,\ \mathbf{E}_2) = \frac{1}{\Omega} \int d\Omega_1\, \rho_1(z,\ \mathbf{E}_2,\ \boldsymbol{\Omega}_1)\, \mathbf{m}_1(\boldsymbol{\Omega}_1) , \tag{2.1}$$

where $\mathbf{m}_1(\boldsymbol{\Omega}_1) = m_1 \hat{s}_1(\boldsymbol{\Omega}_1)$ and Ω is a normalization constant equal to 4π for dipolar hard spheres. Using the invariant expansion (1.9), Eq. (1.13) and the result

$$\int h_{21}^s(z)\, \hat{s}_1(\boldsymbol{\Omega}_1)\, d\boldsymbol{\Omega}_1 = 0$$

we obtain

$$\mathbf{P}(z,\ \mathbf{E}_2) = \frac{m_1 \rho_1^0}{\Omega} \int d\boldsymbol{\Omega}_1 \left\{\left[3K_{21} + \hat{h}_{21}^D(z)\right] D(2,\ 1) + h_{21}^{\Delta}(z)\,\Delta(2,\ 1) + \cdots\right\} \hat{s}_1(\boldsymbol{\Omega}_1) . \tag{2.2}$$

Since

$$\frac{1}{\Omega} \int \hat{s}_1(\boldsymbol{\Omega}_1)\, \hat{s}_1(\boldsymbol{\Omega}_1)\, d\boldsymbol{\Omega}_1 = \tfrac{1}{3}\,\mathbf{U} , \tag{2.3}$$

we have from Eqs. (1.10) and (2.3),

$$\frac{1}{\Omega} \int D(2,\ 1)\, \hat{s}_1(\boldsymbol{\Omega}_1)\, d\boldsymbol{\Omega}_1 = \tfrac{1}{3}(3\cos^2\Theta_2 + 1)^{1/2}\, \hat{e}_2 . \tag{2.4}$$

Also from Eqs. (1.11) and (2.3)

$$\frac{1}{\Omega} \int \Delta(2,\ 1)\, \hat{s}_1(\boldsymbol{\Omega}_1)\, d\boldsymbol{\Omega}_1 = \tfrac{1}{3}\, \hat{s}_2(\boldsymbol{\Omega}_2) = -\tfrac{1}{3}(3\cos^2\Theta_2 + 1)^{1/2}\, \hat{e}_2 + \cos\Theta_2 \hat{n} . \tag{2.5}$$

Using Eqs. (2.4) and (2.5) in Eq. (2.2), eliminating $\hat{h}_{21}^D(z)$ and $h_{21}^{\Delta}(z)$ in favor of the $h_{21}^*(z)$ functions defined through[3]

$$h_{21}^{+}(z) = [\hat{h}_{21}^{D}(z) + \tfrac{1}{2} h_{21}^{\Delta}(z)]/3K_{21} , \quad (2.6)$$

$$h_{21}^{-}(z) = [\hat{h}_{21}^{D}(z) - h_{21}^{\Delta}(z)]/3K_{21} , \quad (2.7)$$

and making use of the relation (1.4) between α and Θ_2 we find

$$\mathbf{P}(z, \mathbf{E}_2) = m_1 \rho_1^0 K_{21}(3\cos^2\Theta_2 + 1)^{1/2}\{[1 + h_{21}^{+}(z) + \cdots]\hat{e}_2 + [h_{21}^{+}(z) - h_{21}^{-}(z) + \cdots]\cos\alpha\hat{n}\} . \quad (2.8)$$

Since

$$\hat{n} = \cos\alpha\hat{e}_2 + \sin\alpha\hat{e}_3 , \quad (2.9)$$

where $(\hat{e}_3, \hat{e}_2)$ form an orthogonal pair of unit vectors,

$$\mathbf{P}(z, \mathbf{E}_2) = m_1\rho_1^0 K_{21}(3\cos^2\Theta_2 + 1)^{1/2} \times\{[1 + h_{21}^{+}(z)\cos^2\alpha + h_{21}^{-}(z)\sin^2\alpha + \cdots]\hat{e}_2 + [h_{21}^{+}(z) - h_{21}^{-}(z) + \cdots]\cos\alpha\sin\alpha\hat{e}_3\} . \quad (2.10)$$

The $h_{21}^{\pm}(z)$ functions are linear combinations of the short-ranged functions $\hat{h}_{21}^{D}(z)$ and $h_{21}^{\Delta}(z)$ and vanish when $z \to \infty$.

Hence,

$$\mathbf{P}(\infty, \mathbf{E}_2) = m_1\rho_1^0 K_{21}(3\cos^2\Theta_2 + 1)^{1/2}\hat{e}_2 , \quad (2.11)$$

which is a relation derived earlier by Rasaiah, Isbister, and Stell.[4] The relationship between K_{21} and $\mathbf{E}_2$ leads, through Eq. (2.11), to the external field dependence of the polarization density at an infinite distance away from the wall.[3,4] Comparing Eqs. (2.10) and (1.6) and taking note of Eq. (2.11), we find that

$$P_2(z, \alpha) = 1 + h_{21}^{+}(z)\cos^2\alpha + h_{21}^{-}(z)\sin^2\alpha + \cdots , \quad (2.12)$$

$$P_3(z, \alpha) = [h_{21}^{+}(z) - h_{21}^{-}(z)](\sin 2\alpha)/2 + \cdots . \quad (2.13)$$

In the MS and LHNC approximations the invariant expansion (1.9) terminates after the first three terms so that Eqs. (2.12) and (2.13) are exact within these approximations. Hence,

$$P_2(z, \alpha) \overset{\text{MS}}{\underset{\text{LHNC}}{=\!=\!=}} 1 + h_{21}^{+}(z)\cos^2\alpha + h_{21}^{-}(z)\sin^2\alpha , \quad (2.14)$$

$$P_3(z, \alpha) \overset{\text{MS}}{\underset{\text{LHNC}}{=\!=\!=}} [h_{21}^{+}(z) - h_{21}^{-}(z)]\frac{\sin 2\alpha}{2} . \quad (2.15)$$

Note that when $\alpha = 0, \pi, \pm\pi/2$, the component $P_3(z, \alpha)$ which is perpendicular to the field vanishes.

III. RESULTS AND DISCUSSION

The formulation of an integral equation for the function $h_{21}^{+}(z)$ and $h_{21}^{-}(z)$ under the MS and RLHNC approximations has been presented in an earlier paper.[3] There the following equation for $h_{21}^{\pm}(z)$ was derived:

$$h_{21}^{\pm}(z) = [g_{21}^{s}(z) - 1] + g_{21}^{s}(z)\,2\pi K_{11}\rho_1^{\pm} \times\{z[B^{\pm}(\infty) - B^{\pm}(z)] + [D^{\pm}(\infty) - D^{\pm}(z)] + \int_0^{\infty} h_{21}^{\pm}(y)[B^{\pm}(\infty) - B^{\pm}(|z - y|)]\,dy\} , \quad (3.1)$$

where K_{11} is related to the dipole moment of the fluid molecules[3] and $B^{\pm}(z)$ and $D^{\pm}(z)$ are integrals over the direct correlation functions $c_{11}^{\pm}(r)$ of fictitous fluids at densities $\rho_1^{+} = 2\rho_1^0$ and $\rho_1^{-} = -\rho_1^0$;

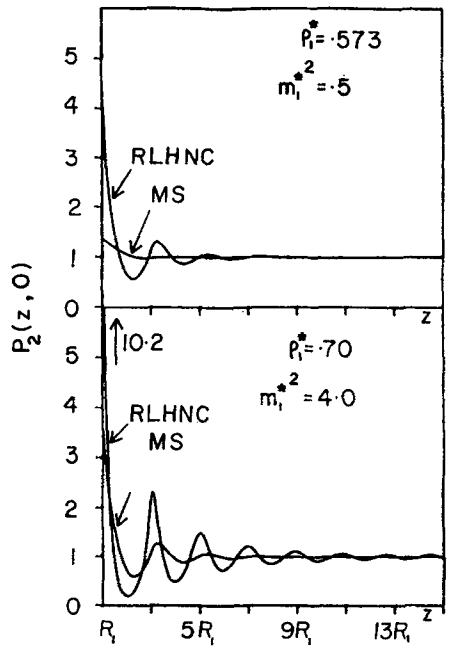

FIG. 2. The component $P_2(z, 0)$ of the polarization density, as a function of distance z from the wall, for models A and B, when $\alpha = 0$. The contact value of $P_2(z, 0)$ in the RLHNC approximation for model B, which has been omitted, is 10.2.

$$B^{\pm}(z) = \int_0^{z} c_{11}^{\pm}(s)\,s\,ds , \quad (3.2)$$

$$D^{\pm}(z) = \int_0^{z} c_{11}^{\pm}(s)\,s^2\,ds . \quad (3.3)$$

When $g_{21}^{s}(z)$ is set equal to 1 in Eq. (3.1) the formal equation for $h_{21}^{\pm}(z)$ in the MS approximation is recovered; otherwise Eq. (3.1) is the appropriate equation to use in the RLHNC approximation.

Solutions of Eq. (3.1) may be applied to the determination of the polarization density profile through Eqs. (2.14) and (2.15). As discussed in Sec. I, the components of $\mathbf{P}(z, \mathbf{E}_2)$, $P_2(z, \alpha)$, and $P_3(z, \alpha)$ are explicitly independent of the electric field and act only to scale the profile about its asymptotic value $\mathbf{P}(\infty, \mathbf{E}_2)$ in the vicinity of the solid–liquid interface. This may be seen in Eq. (3.1) which does not contain any terms which depend explicitly upon the electric field.

The components of the polarization density profile obtained from Eqs. (2.14) and (2.15) are shown in Figs. 2 through 4. Each figure corresponds to a different inclination α of the electric field (see Fig. 1). These calculations are dependent upon two reduced parameters; (1) the reduced density $\rho_1^* = \rho_1^0 R_{11}^3$, where R_{11} is the diameter of bulk hard spheres, and (2) the reduced dipole moment squared $m_1^{*2} = m_1^2/kTR_{11}^3$, where m_1 is the dipole moment, k is Boltzmann's constant, and T is the absolute temperature. Two sets of reduced parameters, displayed in Table I, are used in the calculation presented here. For brevity, we shall refer to these sets as model A and model B. Model B employs nearly the same dipole moment and density as liquid water ($m_1 = 1.85D$) at 295 °K, assuming an effective hard sphere diameter of 2.76 Å. The bulk dielectric con-

TABLE I. Parameters for the model dipolar fluid considered.

Model	ρ_1^*	m_1^{*2}	ϵ(MSA)	ϵ(RLHNC)
A	0.573	0.500	2.67	2.70
B	0.700	4.00	45.8	221

stants, in the limit of zero field, of the two model systems calculated numerically according to the relation[3,7]

$$\epsilon = Q_+(2K_{11}\rho_1^0 R_{11}^3)/Q_-(-K_{11}\rho_1^0 R_{11}^3) , \tag{3.4}$$

where

$$Q_\pm(\rho^\pm) = 1 - \rho^\pm \int c_{11}^\pm(r)\, d\mathbf{r}$$

are also given in Table I. Our results for the MS approximation are in nearly exact agreement with Wertheim's analytic theory,[7] thus providing a useful confirmation of our numerical work for the bulk fluid.

In Fig. 2 the electric field is positioned normal to the surface and the component of the polarization density parallel to the electric field is shown as a function of distance from the wall, in units of the hard sphere radius R_1. As may be seen from Eq. (2.15), the component of the polarization density perpendicular to the field makes no contribution when the electric field is normal to the wall $\alpha = 0$ and $P_2(z, 0)$ is determined by $h_{21}^+(z)$:

$$P_2(z, 0) = 1 + h_{21}^+(z) . \tag{3.5}$$

The upper pair of curves correspond to MS and RLHNC approximations for model A and the lower curves correspond to the higher reduced density and reduced dipole moment of model B.

Several features of $P_2(z, 0)$ are immediately apparent. The nonuniformity of the polarization density for a dense, highly polar fluid is extended further into the bulk phase in the RLHNC approximation. Oscillations in $P_2(z, 0)$, with an amplitude which deviates from its asymptotic value by 5%, are evident beyond even 7 hard sphere diameters from the solid surface for model B. For the same parameters, the MS predicts the bulk polarization density to within 0.001% at roughly 3.5 hard sphere diameters. The upper portion of Fig. 2, $P_2(z, 0)$ for model A, displays the effect of the diminished density and dipole moment which results in a uniform polarization in both theories at around 3.5 hard sphere diameters, with oscillations appearing in the RLHNC approximation which are not present for the MSA. The oscillations in $P_2(z, 0)$ are similar, in some respects, to the polarization density profiles around a single ion in a dipolar solvent.[8]

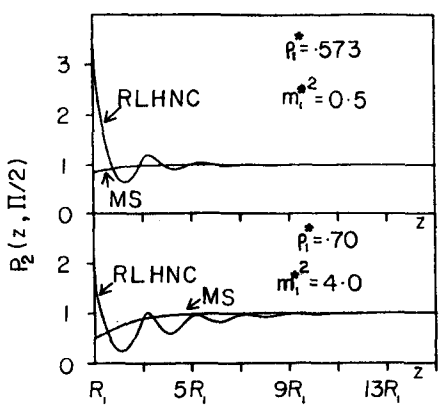

FIG. 3. The component $P_2(z, \pi/2)$ of the polarization density, as a function of distance z from the wall in units of the hard sphere radius, for models A and B when $\alpha = \pi/2$.

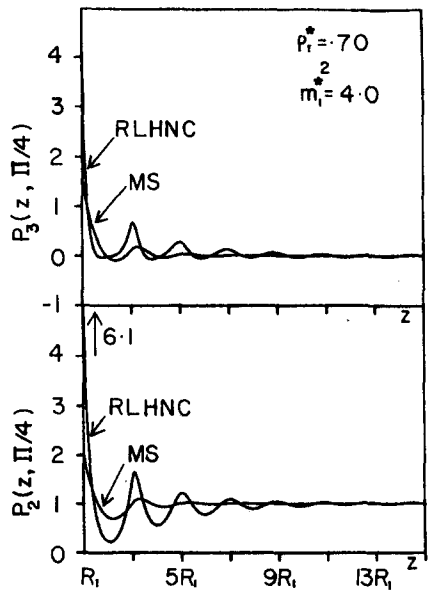

FIG. 4. The components $P_2(z, \pi/4)$ and $P_3(z, \pi/4)$ of the polarization density, as a function of distance z from the wall in units of the hard sphere radius, for models A and B when $\alpha = \pi/4$. The contact value of $P_2(z, \pi/4)$ in the RLHNC approximation, which has been omitted, is 6.1.

When the electric field is parallel to the flat wall, the results of Fig. 3 are obtained. Again $P_3(z, \pi/2)$ makes no contribution to the polarization density. However, for this field orientation the profile is determined by $h_{21}^-(z)$

$$P_2(z, \pi/2) = 1 + h_{21}^-(z) . \tag{3.6}$$

We find again that for model A the asymptotic value of $\mathbf{P}(z, \mathbf{E}_2)$ is attained in 3.5 hard sphere diameters to within 0.001% and that oscillations are extended for model B further into the bulk phase. The effect of lower density and smaller dipole moment are again apparent in the two sets of curves depicted in Fig. 3.

The dependence of $P_2(z, \pi/2)$ on $h_{21}^-(z)$ produces two interesting contrasts. First, the MS approximation produces profiles, similar to bulk $h_{11}^-(r)$ values in this approximation, which rise monotonically to the asymptotic value, unlike profiles in the $\alpha = 0$ case. Second, a field oriented parallel to the wall results in higher polarization densities near contact for model A than for model B, in opposition to the results of Fig. 2, where the field is oriented perpendicular to the wall.

In Fig. 4. we present both components of the polarization density profile produced by a field oriented at 45° from the normal to the wall for parameters which cor-

respond to model B. Both the MS and RLHNC approximations are shown. From Eqs. (2.14) and (2.15) we see that

$$P_2(z,\ \pi/4) = 1 + [h_{21}^{+}(z) + h_{21}^{-}(z)]/2\ , \tag{3.7}$$

$$P_3(z,\ \pi/4) = [h_{21}^{+}(z) - h_{21}^{-}(z)]/2\ . \tag{3.8}$$

Since the $h_{21}^{\pm}(z)$ functions are independent of the magnitude and inclination of the electric field in the MS and RLHNC approximations, $P_2(z,\ \pi/4)$ and $P_3(z,\ \pi/4)$ are linear combinations of $P_2(z,\ 0)$ and $P_2(z,\ \pi/2)$, with

$$P_2(z,\ \pi/4) = [P_2(z,\ 0) + P_2(z,\ \pi/2)]/2\ , \tag{3.9}$$

$$P_3(z,\ \pi/4) = [P_2(z,\ 0) - P_2(z,\ \pi/2)]/2\ . \tag{3.10}$$

Sustained oscillations are present in both components under the RLHNC approximation, whereas the MS closure predicts homogeneity to within 0.001% beyond 3.5 hard sphere diameters. The component $P_3(z,\ \pi/4)$ that lies perpendicular to the electric field vanishes at an infinite distance away from the wall, while $P_2(z,\ \pi/4)$, which lies parallel to the field, has an asymptotic value of unity. It is clear that for any other field angle α that is neither 0 nor $\pi/2$, the components $P_2(z,\ \alpha)$ and $P_3(z,\ \alpha)$ are completely determined, in the LHNC and MS approximations by $P_2(z,\ 0)$, $P_2(z,\ \pi/2)$, and α, all of which are independent of the magnitude of the electric field.

The phase differences between the oscillations of the polarization density profiles predicted by the RLHNC and MS approximations are related to the absence of any contributions to these profiles from the spherically symmetric component of the invariant expansion (1.9) for $h_{21}(z,\ \mathbf{E}_2,\ \Omega_1)$, when the MS approximation is employed. In this approximation, $g_{21}^{s}(z)$ is set equal to unity in the integral equations [Eq. (3.1)] for the $h_{21}^{\pm}(z)$ functions, and the oscillations in $g_{21}^{s}(z)$ near the wall at high densities fail to materialize, with their characteristic phases, in the polarization density profiles even though they are present in the corresponding density profiles. In the RLHNC approximation however, the spherically symmetric component $g_{21}^{s}(z)$ is reflected in the structure of both the density and polarization density profiles.

In their discussion of ion–dipole mixtures using linear response theory, Chan, Mitchell, and Ninham[8] have discussed the separation of the polarization density in Fourier space into components perpendicular and parallel to the **k** direction of the electric field. These components are coupled to the bulk $\tilde{h}_{11}^{+}(k)$ and $\tilde{h}_{11}^{-}(k)$ functions, respectively. Since the Coulomb potential produced by an ion is a longitudinal field, their calculations in the MS approximations deal only with the longitudinal component of the polarization density. Although the electric field created by an ion falls off with distance, a comparison of their work with ours is of interest. When the dielectric constant in the MS approximation is 48, and in the limit of point ions, they obtain negative values of the polarization density near the first two minima. Our calculations, with $\alpha = 0$, would correspond to the opposite limit of a macro-ion producing a constant electric field and do not, for the models and approximations considered here, yield negative values for $P_2(z,\ 0)$.

The circumstances under which the linear constitutive relation is obeyed have already been mentioned in Sec. I and discussed in detail in Ref. 4. Within this linear regime, the polarization density profiles may also be discussed in terms of a local dielectric tensor[9] through an appropriate generalization of the constitutive relation

$$\mathbf{P}(z,\ \mathbf{E}) = \left(\frac{\boldsymbol{\epsilon}(z) - \mathbf{U}}{4\pi}\right) \cdot \mathbf{E}\ , \tag{3.11}$$

where $\boldsymbol{\epsilon}(z)$ is the dielectric tensor and the field **E** is constant. Taking the z axis along the normal $\hat{n}$ and the wall as the xy plane, the off-diagonal elements of the dielectric tensor are zero, with

$$\epsilon_{xx}(z) = \epsilon_{yy}(z) \neq \epsilon_{zz}(z)\ , \tag{3.12}$$

except that

$$\lim_{z\to\infty} \epsilon_{xx}(z) = \lim_{z\to\infty} \epsilon_{zz}(z) = \epsilon\ , \tag{3.13}$$

where ϵ is the bulk dielectric constant. The two independent components may be characterized as the perpendicular and parallel components $\epsilon_{\perp}(z)$ and $\epsilon_{\parallel}(z)$, with reference to the flat wall:

$$\epsilon_{\parallel}(z) = \epsilon_{xx}(z) = \epsilon_{yy}(z)\ , \tag{3.14}$$

$$\epsilon_{\perp}(z) = \epsilon_{zz}(z)\ . \tag{3.15}$$

Orienting the axes so that the field lies in the xz plane, and writing Eq. (3.11) out in detail

$$\mathbf{P}(z,\ \mathbf{E}) = \left(\frac{\epsilon_{\parallel}(z) - 1}{4\pi}\right) E_x \hat{x} + \left(\frac{\epsilon_{\perp}(z) - 1}{4\pi}\right) E_z \hat{n}\ , \tag{3.16}$$

where $\hat{x}$ and $\hat{n}$ are unit vectors along the x and z axes, respectively. Comparison with Eq. (1.6) yields, after some algebra (see Fig. 1)

$$P_2(z,\ \alpha) = 1 + \left(\frac{\epsilon_{\parallel}(z) - 1}{\epsilon - 1} - 1\right) \sin^2\alpha + \left(\frac{\epsilon_{\perp}(z) - 1}{\epsilon - 1} - 1\right) \cos^2\alpha\ , \tag{3.17}$$

$$P_3(z,\ \alpha) = \left(\frac{\epsilon_{\perp}(z) - \epsilon_{\parallel}(z)}{\epsilon - 1}\right) \frac{\sin 2\alpha}{2}\ . \tag{3.18}$$

It follows from Eqs. (2.14) and (2.15) that in the MS and LHNC (or RLHNC) approximations

$$\epsilon_{\perp}(z) = \epsilon + (\epsilon - 1) h_{21}^{+}(z)\ , \tag{3.19}$$

$$\epsilon_{\parallel}(z) = \epsilon + (\epsilon - 1) h_{21}^{-}(z)\ . \tag{3.20}$$

These provide simple relationships between the components of $\boldsymbol{\epsilon}(z)$, the bulk dielectric constant ϵ determined for infinitesimal fields by the particle–particle correlation through Eq. (3.4),[1] and the wall–particle correlations $h_{21}^{\pm}(z)$. It follows from Fig. 2 that near the wall $\epsilon_{\perp}(z)$ is larger than the bulk value. Figure 3, however, implies that $\epsilon_{\parallel}(z)$ behaves quite differently in the vicinity of the wall, in the RLHNC and MS approximations. The local dielectric tensor introduced in our study thus provides a convenient interpretation of the components of the polarization density.

ACKNOWLEDGMENTS

The National Science Foundation and the Australian Research Grants Commission are thanked for their

support of this research. Facilities at the University of Maine Computing Centre are gratefully acknowledged.

[1]For recent reviews see (a) M. S. Wertheim, Annu. Rev. Phys. Chem. **30**, 471 (1979); (b) G. Stell, G. N. Patey, and J. S. Hoye, Adv. Chem. Phys. **48**, 183 (1981).
[2]D. J. Isbister and B. C. Freasier, J. Stat. Phys. **20**, 331 (1979).
[3]J. Eggebrecht, D. J. Isbister, and J. C. Rasaiah, J. Chem. Phys. **73**, 3980 (1980).
[4](a) J. C. Rasaiah, D. J. Isbister, and G. Stell, Chem. Phys. Lett. **79**, 189 (1981); (b) J. C. Rasaiah, D. J. Isbister, and G. Stell, J. Chem. Phys. **75**, 4707 (1981).
[5]S. L. Carnie and D. Y. C. Chan, J. Chem. Phys. **73**, 2944 (1980).
[6]L. Blum and D. Henderson, J. Chem. Phys. **74**, 1902 (1980).
[7]M. Wertheim, J. Chem. Phys. **55**, 4291 (1971).
[8]D. Y. C. Chan, D. J. Mitchell, and B. W. Ninham, J. Chem. Phys. **70**, 2945 (1979).
[9]J. S. Høye and G. Stell, J. Chem. Phys. **72**, 1597 (1980).